

Automatic Detection and Classification of Hypointensity in MR Images of the Brain

R. S. Jasinschi¹, A. Ekin¹, A. C. van Es², J. van der Grond², M. A. van Buchem², A. van Muiswinkel³

¹Video Processing, Philips Research, Eindhoven, Netherlands, ²Department of Radiology, Leiden University Medical Center, Leiden, Netherlands, ³Philips Medical Systems, Best, Netherlands

Synopsis: A method for automated detection and classification of hypointense regions on T2-weighted MR images of the Basal Ganglia (BG) is presented. The detection includes the segmentation of the BG and the use of a normalized feature to detect hypointense regions. We validated our approach by comparing the automated results with a radiologist's assessment of patient data, and found good agreement between these results.

Introduction: An age-related progressive shortening of T2 relaxation time has been described in the BG of normal subjects. In this process the Globus Pallidus becomes hypointense in early adulthood whereas the Putamen is involved after the age of approximately 70 years. This age related increase in signal hypointensity is largely attributed to an increased iron concentration [1]. Excessive deposition of iron has been reported in neurodegenerative diseases like Alzheimer's, Parkinson's, Huntington's disease or in multiple sclerosis. Currently the degree of hypointensity is assessed by visual inspection of T2-weighted (T2-w) images. We propose a fully automated and quantitative method to perform this task. The main components of this method are: (i) segmentation of the BG region [2], (ii) detection of hypointense pixels in the BG, (iii) classification of patients according to the degree of hypointensity. The detection of hypointensity is based on a normalized feature that computes the difference in image brightness between pixels in the BG and in regions containing healthy gray-matter in the cortical ribbon. The classification is based on a measure that counts the number of pixels that are hypointense per unit area. This measure is used to classify patients as severe or almost healthy using a binary decision process.

Methods: We included 42 subjects with atherosclerotic risk factors (mean age $77.4 \pm 3.4y$, 18m/26f). MRI was performed on a Philips Intera 1.5T whole body scanner. We used T1-weighted (TR/TE: 26/12 ms, FLIP: 45°) and dual-spin echo weighted images (TR/TE1/TE2: 3000/27/120 ms, FLIP: 90°) with a FOV 220mm, 3mm slice thickness, no slice gap and 256^2 matrix. The detection was realized in two steps. First, we selected the volume-of-interest (VOI) as described in [3] and the region-of-interest (ROI) corresponding to the midbrain and BG regions, respectively. The original images were skull stripped using the brain extraction tool (BET, version 2), and then a VOI was computed and the brain images in the resulting slices were vertically aligned. A rectangular grid, analogous to the Talairach brain atlas grid defines the ROI. We used a 9 by 8 grid. This allowed us to select anatomically relevant brain areas, such as, the Lenticular Nucleus (Globus Pallidus plus Putamen) in the BG. Second, for each slice in the VOI and for each ROI we computed, per pixel (x, y) , the feature $HypoMR(x, y) = I(x, y) \cdot M / M$, where $I(x, y)$ is the T2-w MRI image brightness, and M is a multiple of m which is the average gray-matter intensity at a grid location containing normal gray-matter in the cortical ribbon. $HypoMR$ varies between 0 (normal signal intensity, low iron) and 1 (low signal intensity, high iron) and it is normalized because of the division by M . We used a gray-matter mask that was obtained from a brain tissue classification method we developed based on harmonic K-means clustering algorithm, to select gray-matter pixels. The classification is based on the degree of hypointensity measure: the percentage of pixels per blocks for which $HypoMR > T$, where T is adaptively determined from the histogram of $HypoMR$. For a set of 16 patients (8 severe, 8 almost healthy), the training set, we computed the average and variance of this measure. These were used for the log likelihood ratio test and to determine the positive (PV+) and negative (PV-) predictive value of the proposed method of the remaining 26 subjects part of the testing set. For the gold standard we used the radiological rating (scoring of the individual BG into iso- or hypo-intense compared to the Globus Pallidus). The latter was performed by two experts in a consensus reading session.

Results: We processed 42 brain MRI volumes. Fig. 1 exemplifies the detection steps of our method. We classified 26 patients as severe (hypointense) or almost healthy (isointense) based on the log likelihood ratio test. Fig. 2 shows the measure used in the patient classification. Our method yielded a PV+ of 0.88 and a PV- of 0.78.

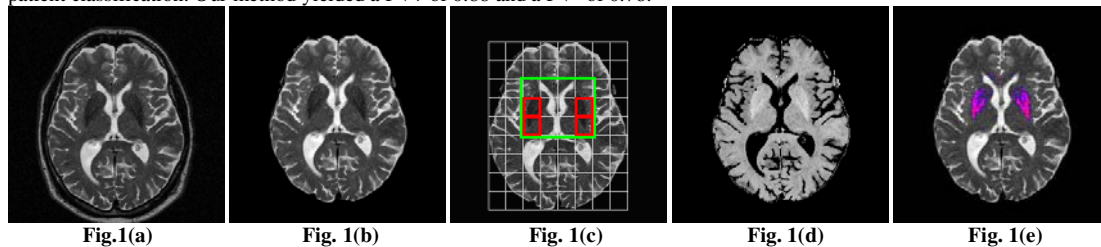


Fig. 1: The original T2-w MRI in 1(a), its skull stripped and vertically aligned brain image in 1(b), the 8 by 9 rectangular grid superimposed on image 1(b) in 1(c); the green rectangle in 1(c) is the ROI and the four red blocks include large areas of the Lenticular Nucleus. The image of the $HypoMR$ feature, normalized and scaled from 1 to 255 is shown in 1(d). Fig 1(e) shows the pixels (Lenticular Nucleus) with $HypoMR > 0.70$. Pixels in light purple are more hypointense than the pixels in blue.

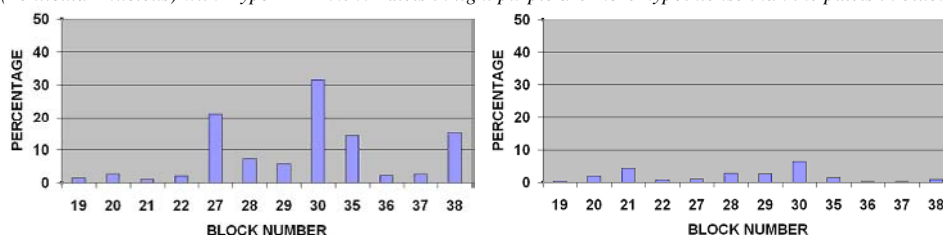


Fig. 2: The pixel percentage per unit area for which $HypoMR > 0.70$, in subjects who were radiologically graded as having hypointense BG (left) and isointense BG (right). The blocks are numbered in raster scan order, from top left to bottom right, so that Block 1 is top left and Block 72 bottom right. For patients having hypointense BG Blocks 27, 30, 35 and 38, shown in red in Fig. 1(c), correspond to large parts of the Lenticular Nucleus and they have the highest percentage of hypointense pixels.

Conclusion: This proposed method computes pixel accurate values of hypointensity for T2-w MRI images that is normalized across slices and volumes. A fast and robust implementation of it could be used in the scanning and diagnosing of patients.

[1] Gregory A.M., et al <http://www.orpha.net/data/patho/GB/uk-NBIA.pdf>.

[2] Linguraru M.G., et al <ftp://ftp-sop.inria.fr/epidaure/Publications/Gonzalez/Linguraru:Acta:2004.pdf>.

[3] Ekin A. et al., Fast, Shape-directed, Landmark-based Deep Gray Matter Segm. for Quant. of Iron Deposition, SPIE 2006.

Confidentiality Notice: Please note that this paper/abstract is sent to you for the purpose of reviewing only, and that it is to remain strictly confidential until it is actually published in the workshop/conference proceedings, on or after the official pre-announced date of public availability on the website of the workshop/conference. You should not pass it on or disclose its contents to anyone else, except when you delegate the reviewing to other reviewers, in which case it remains your responsibility to ensure that the other reviewers observe the same strict confidentiality.